

# Production and Characterization of Al-TiB<sub>2</sub>-ZrB<sub>2</sub> Hybrid Composite Using In-situ Stir Casting Process

Rajakumar S. Rai<sup>1</sup>, J. David Rathnaraj<sup>2</sup>

<sup>1</sup> Assistant Professor, Department of Mechanical Engineering, Karunya University, Coimbatore

<sup>2</sup> Professor, Department of Manufacturing Engineering, Sri Ramakrishna Engineering College, Coimbatore

**Corresponding author:**

Rajakumar S. Rai, Assistant Professor, Department of Mechanical Engineering, Karunya University, Coimbatore, INDIA, Pin Code: 641114

Email: rajakumars@karunya.edu; Mobile No.: +91 9940985882

**Abstract-** In the present work, a hybrid metal matrix composite with Aluminum, Titanium di-boride and Zirconium di-boride was produced using in-situ stir casting process. The composites were characterized for their metallurgical and mechanical properties. The XRD results revealed the presence of the reinforcement particles in the metal matrix. The SEM microstructures showed the homogeneous distribution of the reinforcement particles in the aluminum matrix. The microhardness test confirmed the improvement in the mechanical property of the composites and showed a 33% increase in microhardness, for Al – 3 wt.% TiB<sub>2</sub> – 7 wt.% ZrB<sub>2</sub>MMC when compared to the as cast AA6061.

**Keywords-** Hybrid Metal Matrix Composite, Metallurgical characterization, XRD, SEM, Micro hardness

## 1. Introduction

Composites have always excited researchers around the globe. Metal matrix composites (MMCs) have recently replaced their monolithic counterparts in various applications [1-3]. The success of MMCs has paved way for the development of hybrid MMCs. The prospective applications are plenty if a hybrid property can be achieved through these hybrid composites.

The primary issue in manufacturing MMCs is with the process itself. Researchers have tried various methods to produce them [4-6]. The most commonly used process is stir casting process. In this process, the matrix material is heated in a furnace until the material melts. Then the reinforcing material is added to the melt either in powder form which is termed as ex-situ process or adding chemicals which react in the melt and produces the required reinforcing material as a result of the reaction. This method is termed as in-situ process. The major issue of ex-situ process is the wettability of the reinforcing particles in the melt. The ability of it to mix in the molten metal can be enhanced by using wetting agents like Magnesium (Mg) or Potassium Titanium Fluoride (K<sub>2</sub>TiF<sub>6</sub>) [7-9]. Though various procedures are followed by researchers they have always found it difficult to cast a sound MMC using ex-situ process [10-12]. Many researchers have proved that this problem can be completely eliminated by in-situ process [14-18]. Since more than one particle was used

as reinforcement, in-situ process was selected for producing these MMCs.

In the present work MMCs were produced with Aluminum (AA6061) as the matrix material. Titanium di-Boride (TiB<sub>2</sub>) and Zirconium di-Boride (ZrB<sub>2</sub>) were added as reinforcements. AA6061 is a structural material and finds application in aerospace, automobile and marine structures. TiB<sub>2</sub> and ZrB<sub>2</sub> are hard ceramic materials and are the commonly used reinforcements in MMCs. Researchers have proved that by adding these reinforcements, there has been improvements in the mechanical and metallurgical properties of MMCs to a large extent [19-23]. Since these two materials were produced using similar chemicals in in-situ process, they complement well with each other and the process parameters were the same for producing the MMCs. Thus these two ceramic particles were added together in in-situ form to produce the hybrid composites.

A detailed metallurgical characterization was carried out using optical micrograph and SEM, on the produced MMCs, to verify their properties and characteristics. XRD analysis was carried out to evaluate the presence of reinforcing particles and also to verify the presence of intermetallic phases which might have formed during in-situ process. Microhardness survey was also done on the MMCs to evaluate the change in the mechanical properties for different combinations of MMCs.

## 2. Experimental Procedure

### *Fabrication of Composite*

Three different combinations of Al-TiB<sub>2</sub>-ZrB<sub>2</sub>MMCs were fabricated as presented in Table 1. Figure 1 shows the indigenously developed stir casting furnace which was used to fabricate the MMCs. The chemical composition of aluminum alloy (AA6061-T6) which was used as the matrix material is given in Table 2.

Table 1. Combinations of MMCs Produced

Sl. No.	Wt.% of AA6061	Wt.% of TiB <sub>2</sub>	Wt.% of ZrB <sub>2</sub>
1.	90	5	5
2.	90	3	7
3.	90	7	3

Table 2. Chemical Composition of AA6061-T6

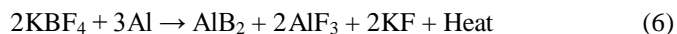
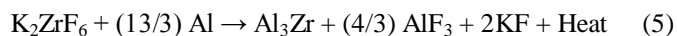
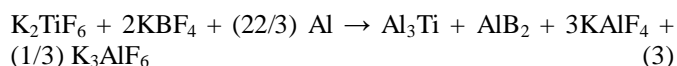
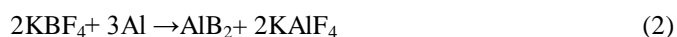
Elements	Mg	Si	Fe	Cu	Mn	Cr	Zn	Ti	Al
% by weight	0.95	0.54	0.22	0.17	0.13	0.09	0.08	0.01	Balance

The primary objective in fabricating MMCs using in-situ technique is to identify the chemicals and its stoichiometric ratio. To fabricate this composite, the chemicals that were used are  $K_2TiF_6$ ,  $K_2ZrF_6$  and  $KBF_4$  [13].



Fig 1. Typical Stir Casting Furnace showing the Stirrer in Operation.

Equations 1, 2, 3 and 4 describe the chemicals that were used to obtain  $TiB_2$  particles in the melt and the chemical reaction that happens during the process. Equation 5, 6 and 7 describe the same for obtaining  $ZrB_2$  particles in the melt.



It is essential to maintain a proper stoichiometric ratio to enable the reaction to complete and to avoid the formation of intermetallic components like  $Al_3Ti$  or  $Al_3Zr$ . The amount of chemicals to be added to the melt is determined by this stoichiometric ratio. The values are calculated using atomic weight of each component in the chemical and the weight of the total casting.

Table 3. Amount of Chemicals used for MMC Combinations

Sl. No.	To obtain $TiB_2$		To obtain $ZrB_2$	
	$K_2TiF_6$ (gms)	$KBF_4$ (gms)	$K_2ZrF_6$ (gms)	$KBF_4$ (gms)
1.	154.76	162.34	112.50	99.95
2.	154.76	162.34	173.54	154.17
3.	233.73	245.17	72.82	64.69

When compared to the calculated value of the chemicals, a 10 wt. % of extra chemicals was added to compensate for the losses during the casting process, in terms of slag and oxides. Table 3 shows the amount of chemicals used for various combinations of MMCs.

The furnace was heated up to  $700^\circ C$  before the aluminum rods were kept in the graphite crucible. The crucible was coated with wolfrakoat – a non-reactive coating to prevent reaction between the crucible and aluminum melt. Once the aluminum rod melts and the temperature reaches to  $850^\circ C$ , the chemicals were added to the melt in the form of capsules packed in aluminum foil. The melt and chemicals were left idle for reaction to initiate for 20 minutes. After that the melt is intermittently stirred using a mechanical stirrer for every 10 minutes, at 350 rpm for 40 minutes. Once the reaction is complete and visually there are no sparks coming out of the melt, the slag which floats over the melt is removed using a steel ladle. Then the final stirring is done and the melt is poured inside the steel die to obtain the required shape. Manual stirring is continued until the melt is poured inside the die. Figure 2 shows the cast composites for the 3 combinations said above.



Fig 2. Cast plate of Al- $TiB_2$ - $ZrB_2$  MMC

#### Metallurgical Characterization

Specimens were extracted from the cast composite to conduct various tests. A 3 mm thick plate of 20 mm x 20 mm size was cut using wire cut EDM process for XRD analysis of the specimen. A 6 mm x 6 mm x 30 mm rod was cut from the composite to conduct the SEM analysis and Microhardness test. The specimen was prepared using standard metallographic procedure and etched using Keller's reagent followed by Weck's reagent. XRD analysis was conducted

using Jeol XRD Analyzer, SEM analysis was conducted using Shimadzu machine and microhardness test was conducted using Mitutoyo machine.

### 3. Result and Discussion

#### XRD analysis

Figure 3 to 5 shows the XRD results of the cast composite. Figure 3 shows the result of the first casting where the reinforcement particles were equally added and it was found that the XRD plot revealed the presence of these reinforcements in the metal matrix. The peaks of the reinforcements were very small and not prominent because of the reason that the intensity of the diffractions was not high enough. This is because the specimen which was used might have lesser particle distribution. Nevertheless, it showed a glimpse of the presence of the particles. A more clear analysis was carried out using SEM and the presence of  $TiB_2$  and  $ZrB_2$  were confirmed.

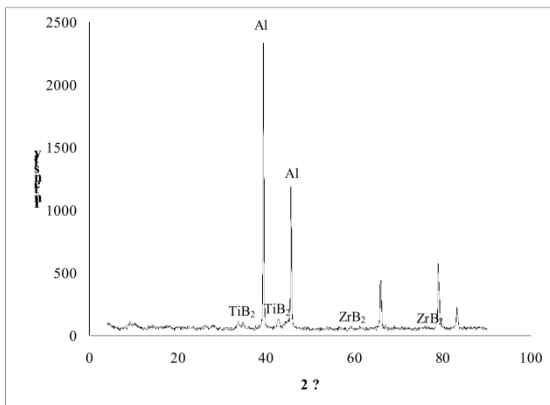


Fig 3. XRD Results of  $Al - 5 \text{ wt. } \% TiB_2 - 5 \text{ wt. } \% ZrB_2$  MMC

Figure 4 shows the results of the second casting. The presence of the reinforcement particles were revealed clearly in the plot. The intensity of the peaks are high enough to show their presence. But when the plot is clearly examined, it had an erratic pattern showing the presence of some slags of potassium and fluoride. Since the XRD specimens were cut from the top surface of the casting, it is found that some amount of this slag is trapped inside the casting at the raiser location.

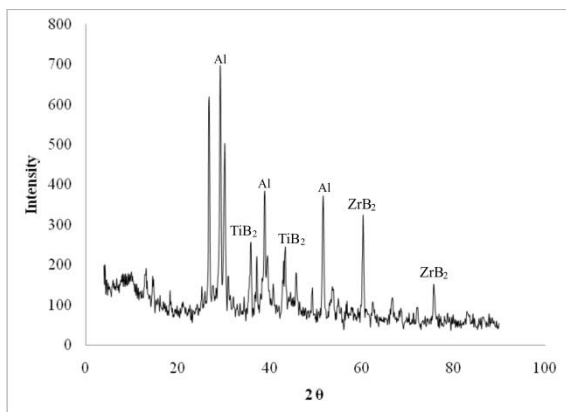


Fig 4. XRD Results of  $Al - 3 \text{ wt. } \% TiB_2 - 7 \text{ wt. } \% ZrB_2$  MMC

Figure 5 shows the results of the third casting. Here also a similar kind of plot is visible. The XRD plot not only revealed the presence of the reinforcement particles but also the presence of slag in some amount. Since it was the defect caused during the manufacturing process, the specimen for SEM were taken from the bottom of the cast plate which did not show any traces of these slag entrapment in that location.

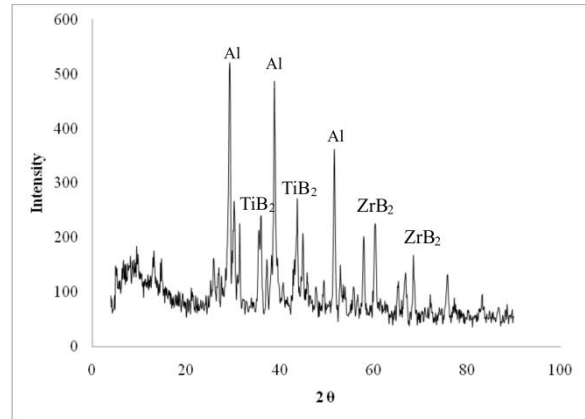


Fig 5. XRD Results of  $Al - 7 \text{ wt. } \% TiB_2 - 3 \text{ wt. } \% ZrB_2$  MMC

#### SEM analysis

The SEM micrograph in Figure 6 reveals the presence of both the reinforcement particles  $ZrB_2$  and  $TiB_2$  in clusters in the  $Al - 5 \text{ wt. } \% TiB_2 - 5 \text{ wt. } \% ZrB_2$  MMC. Figure 7 and Figure 8 show the higher magnification images of the particles for the same MMC. As mentioned in literatures, the  $ZrB_2$  particles are in the form of irregular shapes. A few particles are in spherical shape as well. The  $TiB_2$  particles are in the form of spherical shape and a few are hexagonal in shape. The figures also reveal that the particles are uneven in size and they vary between  $2\mu$  to  $5\mu$  in the matrix. This phenomenon is also reported in literatures. The reason for this uneven particles size is due to the in-situ fabrication technique where the chemical salts react between them in different quantities and for the required reinforcement particle. Therefore there are variations in the particle size. Though the figures show that the particles are in clusters in few places, figure 6 shows that the particles are also distributed across the matrix homogeneously. This shows that the stirring action of the impeller has propelled the particles in the melt and made them to settle in the matrix, and is evenly distributed.

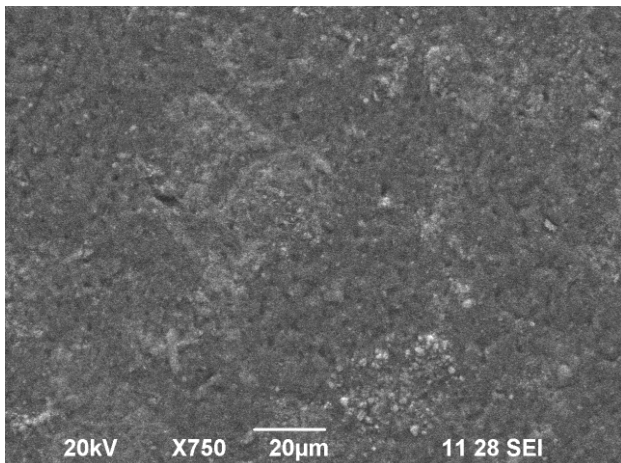


Fig 6. SEM micrograph showing the presence of  $TiB_2$  and  $ZrB_2$  particles in  $Al - 5 \text{ wt.}\% TiB_2 - 5 \text{ wt.}\% ZrB_2$  MMC

Figure 9 shows the SEM micrograph of  $Al - 3 \text{ wt.}\% TiB_2 - 7 \text{ wt.}\% ZrB_2$  MMC. The microstructure reveals that the  $ZrB_2$  particles are homogeneously distributed across the Al matrix. It also shows some small clusters of agglomeration of reinforcement particles in the matrix. Figure 10 shows the higher magnification of the MMC and it clearly shows the irregular shaped  $ZrB_2$  particles. The particle size of  $2.5\mu$  is seen in the microstructure.

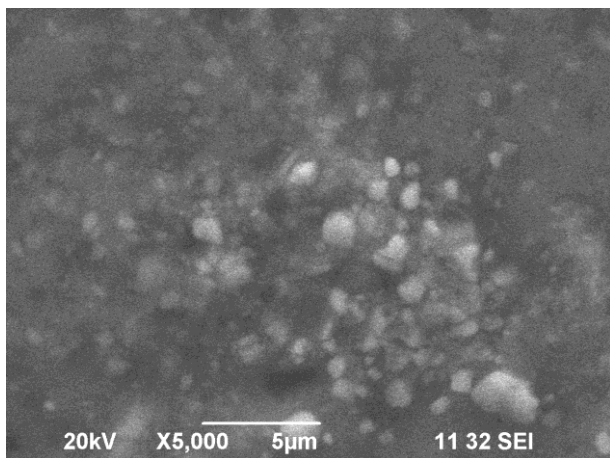


Fig 7. SEM micrograph showing  $ZrB_2$  particles in  $Al - 5 \text{ wt.}\% TiB_2 - 5 \text{ wt.}\% ZrB_2$  MMC

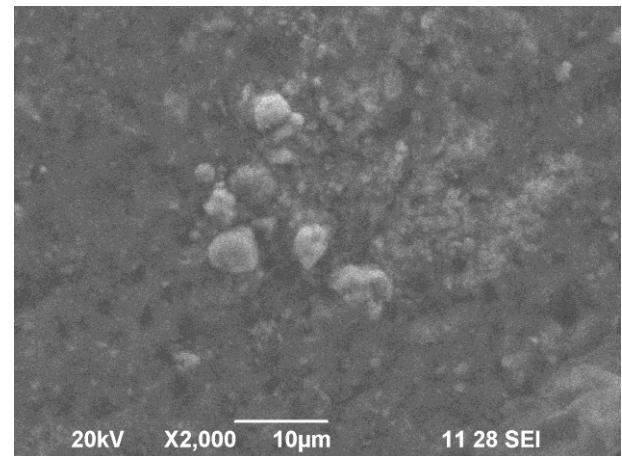


Fig 8. SEM micrograph showing  $TiB_2$  particles in  $Al - 5 \text{ wt.}\% TiB_2 - 5 \text{ wt.}\% ZrB_2$  MMC

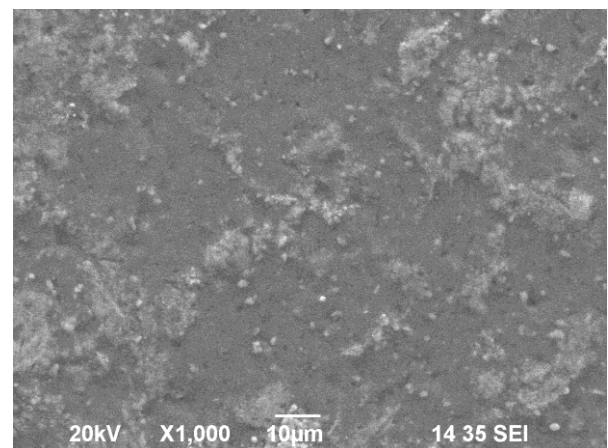


Fig 9. SEM micrograph showing the presence of  $TiB_2$  and  $ZrB_2$  particles in  $Al - 3 \text{ wt.}\% TiB_2 - 7 \text{ wt.}\% ZrB_2$  MMC

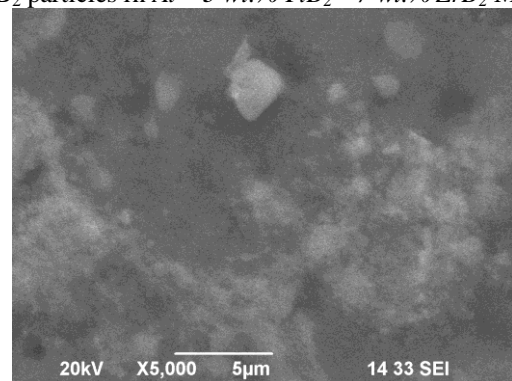


Figure 10. SEM micrograph showing  $ZrB_2$  particles in  $Al - 3 \text{ wt.}\% TiB_2 - 7 \text{ wt.}\% ZrB_2$  MMC

Figure 11 shows the SEM micrograph of  $Al - 7 \text{ wt.}\% TiB_2 - 3 \text{ wt.}\% ZrB_2$  MMC. From the figure it is evident that  $TiB_2$  particles are present in the matrix in the form of large agglomerations. The microstructure also shows the dendritic structure of the cast aluminum composite. A higher magnification in figure 12 shows the presence of spherical shaped  $TiB_2$  particle of  $5\mu$  size, in the matrix. A very few  $ZrB_2$  particles are identified in the matrix. This may be due to the less wt.% of  $ZrB_2$  that is used in the MMC.

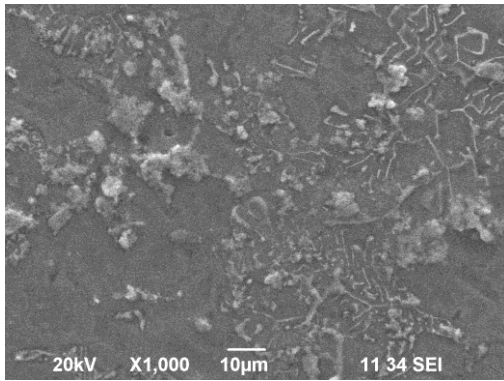


Fig 11. SEM micrograph showing the presence of  $TiB_2$  and  $ZrB_2$  particles in  $Al - 7 \text{ wt.}\% TiB_2 - 3 \text{ wt.}\% ZrB_2$  MMC

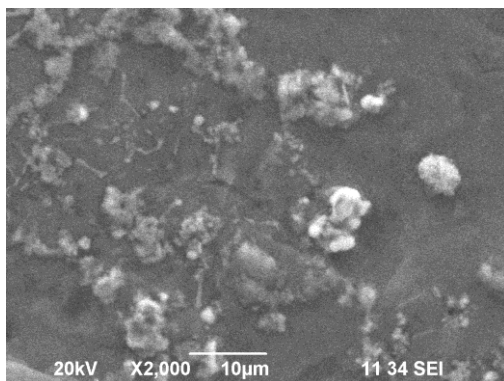


Fig 12. SEM micrograph showing  $TiB_2$  particles in  $Al - 7 \text{ wt.}\% TiB_2 - 3 \text{ wt.}\% ZrB_2$  MMC

#### Micro hardness Test

The micro hardness values for the three different castings are presented in table 4. The table clearly shows the increase in the hardness values when compared to the as cast AA6061. The table also shows that the hardness values is higher for MMC with  $Al - 7 \text{ wt.}\% TiB_2 - 3 \text{ wt.}\% ZrB_2$  combination, when compared to the other two castings. This is because of the presence of  $TiB_2$  particles in large number and they exhibit more resistance to the indenter than the  $ZrB_2$  particles, and hence the property.

Table 4. Micro hardness values of as cast Aluminum and MMCs

Sl. No.	Material Combination	Microhardness Value (HV)
1.	As cast AA6061	120
2.	$Al - 5 \text{ wt.}\% TiB_2 - 5 \text{ wt.}\% ZrB_2$ MMC	140
3.	$Al - 3 \text{ wt.}\% TiB_2 - 7 \text{ wt.}\% ZrB_2$ MMC	132
4.	$Al - 7 \text{ wt.}\% TiB_2 - 3 \text{ wt.}\% ZrB_2$ MMC	160

The composite, which has equal amount of these particles, exhibit a slightly increased hardness value than the one with more  $ZrB_2$  particles. This is because of the presence of  $TiB_2$  particles in the matrix. Therefore the table clearly shows that the combination of these particles have certainly improved the property of the material.

#### 4. Conclusion

The following are the conclusions based on the work carried out thus far.

- In-situ stir casting procedure is one of the successful methods to produce hybrid metal matrix composites.
- The XRD results clearly showed the presence of the reinforcement particles in the aluminum matrix.
- The SEM results also showed that the reinforcement particles were evenly distributed in the metal matrix and exhibited a homogeneous property across the cast plate.
- The microhardness test showed that there is up to 33% increase in the hardness for the specified percentage reinforcement of  $TiB_2$  and  $ZrB_2$  particles.

#### Acknowledgement

The authors wish to acknowledge the Centre for Research in Metallurgy (CRM), Department of Mechanical Engineering, Karunya University and Department of Nanotechnology, Karunya University for providing all the fabricating and testing facilities to conduct the experiments.

#### References

- [1] Suraj,P. Rawal,; JOM,53(4), 2001, p. 14.
- [2] Evans, A.,Marchi, C. S., Mortensen,A.: Metal matrix composites in industry: an introduction and a survey. Netherlands, Kluwer Academic Publishers 2003.
- [3.] Oroño,J.: Rare metals, 30(2), 2011, p.200.
- [4] Miracle,D.B.: Composite Science and Technology, 65, 2005, p. 2526.
- [5] Hunt, W.H.: In: Proceedings Processing and Fabrication of Advanced Materials III, TMS, 1994, p. 663.
- [6] Olivares Santiago,M., GalánMavín, C., RoaFernández,J.: Informes de la Construcción, 54, 2003, p. 484.
- [7] Hashim, J., Looney, L., Hashmi,M.S.J.: J. of Mater. Proc. Tech., 123, 2002, p. 251.
- [8] Warren H. Hunt: Mater. Sci. Forum, 331, 2000, p. 71.
- [9] Banerji, A.,Rohatgi,P. K.: J. of Mater. Sci., 17,1982, p. 335.
- [10] David L. McDanel,;Metall. Trans. A.,16(6), 1985, p. 1105.
- [11] Feng, C. F., Froyen,L.: J. of Mater.Sci., 35, 2000, p. 837.
- [12] Kennedy, A. R.,Karantzalis, A. E.,Wayatt,S. M.: Journal of Mater.Sci.,34, 1999, p. 933.
- [13] Christy, T. V.,Murugan, N., Kumar,S.: J. of Miner. Mater.Charac.Engg.,1,2010, p. 57.
- [14] Gurcan, A. B.,Barker. T. N.:Wear, 188(1), 1995, p. 185.
- [15] Degang Zhao,Xiangfa Liu, Yuxian Liu, XiufangBian,; J.of Mater.Sci.,40, 2005, p. 4356.
- [16] Cambronero,L. E. G., Ruiz-Roman, J. M.,Ruiz Prieto, J. M.,Salvador,M. D.:In: ProceedingsVIII Congreso Nacional de propiedades Mecánicas de Sólidos, Gandia 2002, p. 107.

- [17] Feng, C. F.,Froyen,L.:ActaMater.,47(18), 1999, p. 4571.
- [18] Kaczumar, J. W.,Pietrzak, K., Wlosinski, W.: J. of Mater. Proc. Tech., 106, 2000, p. 58.
- [19] Fogagnolo, J. B.,Robert, M. H.,Ruiz-Navas, E. M.,Torralba,J. M.: J.Mater. Sci.,39, 2004, p. 127.
- [20] Fogagnolo, J. B.,Robert, M. H.,Velasco, F., Torralba,J. M.: Kona, 22, 2004, p. 515.
- [21] Pai,B.C., GeethaRamani, Pillai, R. M.,Satyanarayana,K. G.: J. of Mater.Sci.,30, 1995, p. 1903.
- [22] Hashim, J., Looney, L., Hashmi,M.S.J.: J. of Mater. Proc. Tech.,92, 1999, p. 1.
- [23] Rosso,M.:J. of Mater. Proc. Tech.,175, 2006, p. 364.